Low-energy electron scattering from BCl_3

W. A. Isaacs and C. W. McCurdy
Computing Sciences, Lawrence Berkeley National Laboratory, Berkeley, California 94720

T. N. Rescigno
Physics and Space Technology Directorate, Lawrence Livermore National Laboratory, Livermore, California 94550

(Received 8 April 1998)

Despite the importance of BCl_3 in plasmas used for commercial etching processes, no calculations or measurements of elastic low-energy electron scattering from BCl_3 have previously appeared in the literature. We therefore present calculations based on the complex Kohn method for elastic electron-BCl_3 scattering at incident electron energies below 8 eV. We find a near-zero-energy virtual state and a sharp temporary negative-ion resonance at 0.25 eV, which likely contributes to the large electron attachment cross sections observed in swarm studies. [S1050-2947(98)03410-6]

PACS number(s): 34.80.Bm

I. INTRODUCTION

Boron trichloride (BCl_3) is a common component of plasmas used in the commercial etching of both semiconductors and metals [1–4]. The modeling of such plasmas is a challenging task, made even more difficult by the scarcity of data on basic atomic and molecular processes involving BCl_3 and its fragments. Plasma conditions are such that free electrons have energies in the few-eV range and these low-energy electrons initiate much of the plasma chemistry.

The highly reactive nature of BCl_3 that makes it so attractive as an etchant makes it particularly unattractive as a target in a crossed electron-molecular beam apparatus. There have been a few studies [5,6] of electron impact dissociation of BCl_3 in this configuration, but all have found BCl_3 pressures as low as 10^{-6} Torr problematic, requiring the *in situ* monitoring of N_2 dissociation to calibrate for contact potential drift. It seems unlikely that low-energy elastic electron BCl_3 measurements under single collision conditions will soon be feasible. Thus, most of the experimental information on electron-BCl_3 scattering has been obtained indirectly from cell or swarm experiments [7–14]. Nagpal and Garscadden [8] have extracted inelastic cross sections from electron drift velocity measurements [9] of BCl_3/Ar and BCl_3/He mixtures for a wide range of E/N (where E is the electric field and N is the gas number density). To minimize the effects of electron attachment to BCl_3, a process known to have a large cross section [11,13,14], the measurements were taken at very low concentrations of BCl_3. These conditions precluded unfolding the elastic momentum transfer cross section, though vibrational excitation and dissociation cross sections consistent with the observed drift velocity data were obtained.

The ion chemistry in BCl_3 discharges is rich [10]. Ionization and dissociative ionization cross sections have recently been obtained by Fourier-transform mass spectrometry [7]. The production of Cl^- by dissociative electron attachment (DA) has been measured and observed to peak at a scattering energy of 1.1 eV [13]. Observations of BCl_3^- are consistent with a large attachment cross section peaked near zero energy and a very long autodetachment lifetime (the estimate 60 microseconds has been suggested [14,15], similar to the well known case of SF_6^-). To our knowledge, there are no published electron scattering calculations on BCl_3.

The recent study of Baeck and Bartlett [16] on the structure of the boron chlorides provides a necessary base of knowledge that will prove important in the future modeling of BCl_3 plasmas. In view of the importance of the complementary scattering information, we have performed *ab initio* calculations of elastic electron-BCl_3 scattering in the 0.05–8 eV energy range. We have used the complex Kohn variational method and have accounted for the effects of target relaxation through the use of polarized orbitals, and by a relaxed-SCF (self-consistent field) treatment of the temporary negative-ion resonance. Section II contains a brief description of the theoretical method. In Sec. III we present the details of the calculations and their results, and offer some concluding comments on dissociative attachment in Sec. IV.

II. COMPLEX KOHN VARIATIONAL METHOD

Detailed descriptions of the complex Kohn variational method [17,18] have been presented elsewhere; only a summary will be given here. This work was restricted to a consideration of electronically elastic scattering; thus, we used a trial wave function of the form

$$\Psi_t(\mathbf{r}_1\cdots\mathbf{r}_{N+1}) = A(\chi_o(\mathbf{r}_1\cdots\mathbf{r}_N)F(\mathbf{r}_{N+1})) + \sum_i d_i\Theta_i(\mathbf{r}_1\cdots\mathbf{r}_{N+1}), \quad (1)$$

where F is the function that describes the scattered electron, χ_0 is the target wave function, and A is the antisymmetrization operator. The single particle continuum function F is further expanded as

$$F(\mathbf{r}) = \sum_{lm} [f_l(r)\delta_{ll'}\delta_{mm'} + T_{lml'm'}g_l(r)]Y_{lm}(\hat{\mathbf{r}})/r + \sum_k c_k\phi_k(\mathbf{r}) \quad (2)$$

in a basis of symmetry-adapted molecular orbitals $\phi_k(\mathbf{r})$, along with products of spherical harmonics $Y_{lm}(\hat{\mathbf{r}})$ and both regular (Ricatti-Bessel) and complex outgoing continuum functions [$f_l(r)$ and $g_l(r)$, respectively] to enforce the required asymptotic boundary conditions. The partial wave components of the transition matrix $T_{lml'm'}$ are obtained by solving a set of linear equations derived from a stationary principle for the T matrix.

The $(N+1)$-electron configurations Θ_i represent the polarization and correlation due to closed channels. Because these square-integrable configurations do not explicitly participate in the determination of the scattering matrix, it is convenient to use Feshbach partitioning [19] to separate the trial wave function into two terms, $P\Psi$ and $Q\Psi$, corresponding to the two terms on the right side of Eq. (1). Defining M as $(H-E)$, we can write an effective Hamiltonian [17] that determines $P\Psi$:

$$H_{\text{eff}}=H_{PP}-M_{PQ}\,\frac{1}{E-H_{QQ}}\,M_{QP}=H_{PP}-V_{\text{opt}}. \qquad (3)$$

The optical potential V_{opt} compactly incorporates the correlation effects of the closed channels.

The importance of polarization effects in low-energy electron molecule scattering has been shown in numerous studies, for example in electron scattering from methane [20], silane [21], and, most recently, carbon tetrafluoride [22]. In each of these systems an accurate account of the effects of closed channels is necessary to reproduce the position of the observed Ramsauer-Townsend (RT) minimum. The polarizability of these systems was accurately described by using an SCF wave function for the target ground state and constructing the $(N+1)$-electron terms, Θ_i, in the trial wave function as products of bound molecular orbitals and terms obtained by singly exciting the target SCF wave function into a set of ''polarized'' orbitals. While we do not necessarily expect BCl_3 to possess a RT minimum, we would nevertheless expect that for a nonpolar molecule such as BCl_3 the low-energy cross section is sensitive to the dynamic polarization of the target by the incident electron; the ''polarized-SCF'' model has been shown to give an accurate description of this effect.

Besides RT minima, another common feature of low-energy electron-molecule scattering is the temporary negative-ion shape resonance. When these resonances occur at low energy, their positions and lifetimes can be quite sensitive to the inclusion of short-range $(N+1)$-electron correlation. The dominant effect that must be described in this case is the dynamic distortion of the target wave function in the presence of the scattering electron. In describing this effect, we must take some care to maintain a balanced treatment of correlation in the N- and $(N+1)$-electron systems. For target molecules such as N_2 [23], H_2CO [24], and C_2H_4 [25], which all possess low-energy negative-ion shape resonances, it has been shown that the most important configurations to include are those particle-hole target excitations that preserve spatial symmetry. As we will discuss in the following section, we found that both types of correlation effects (target polarization involving optically allowed closed channels and target distortion involving configurations that preserve the symmetry of the ground state) are important in e^--BCl_3 elastic scattering.

Applications of *ab initio* methods to electron scattering by molecular targets composed of atoms with more than a few electrons can be considerably simplified by using effective core potentials (ECP's) to replace the inner shell target electrons, which act primarily as spectators in the scattering event. Natelense *et al.* [26] have demonstrated the utility of ECP's by carrying out electron scattering calculations at the static-exchange level on a series of tetrahedral molecules using norm-conserving pseudopotentials. For the case of CF_4, they showed that such calculations produce cross sections that differ insignificantly from those obtained in an all-electron treatment. We have previously shown how ECP's can be incorporated into the Kohn method [27] and reported the results of calculations on HBr [28], CH_3Cl [29], and CF_4 [22] that used this technique. Our work here employs the ECP's of Pacios and Christiansen [30] to replace the $1s$, $2s$, and $2p$ electrons of the chlorines. Using ECP's reduces the number of active electrons in the calculation from 56 to 26, and results in a substantial savings of computational effort with minimal expected effect on the final results.

III. CALCULATIONS

All calculations were performed at the equilibrium D_{3h} geometry with $R_{(\text{B-Cl})}=1.754$ Å [16]. Because our molecular structure codes are limited to the use of Abelian point groups, we employed the (lower) symmetry C_{2v}. All symmetry labels presented here will be C_{2v} unless otherwise noted.

To compute the target SCF wave function, we used a contracted $(9s5p1d)/[5s3p1d]$ Gaussian basis [31] for boron, and employed the uncontracted $[4s4p]$ Gaussian basis sets given by Pacios and Christiansen [30] for chlorine along with their effective potentials to replace the atomic $n=1$ and 2 cores. For the purpose of generating a set of polarized orbitals and for constructing the Kohn trial wave function, the target basis was augmented with additional functions. On the boron atom, we used four additional s functions with exponents 0.039, 0.015, 0.006, and 0.002 and two p functions with exponents 0.025 and 0.009; on each of the chlorines we added p functions with exponents 1.6 and 0.065 and two d functions with exponents 0.5 and 0.17. This prescription generated a basis of 132 functions. To complete the expansion of the trial scattering function, we included numerically generated continuum functions [32], retaining terms with angular momentum l less than or equal to 5. Total and momentum transfer cross sections were calculated with contributions from these partial waves.

A. Static exchange

The static-exchange (SE) approximation neglects all target relaxation effects, i.e., no $(N+1)$-electron configurations Θ_i are included in Eq. (1). This level of approximation is well known to be quantitatively, and often qualitatively, incorrect at scattering energies of a few eV and less, but generally displays the basic features of the scattering. The SE level also provides a baseline for comparison with future

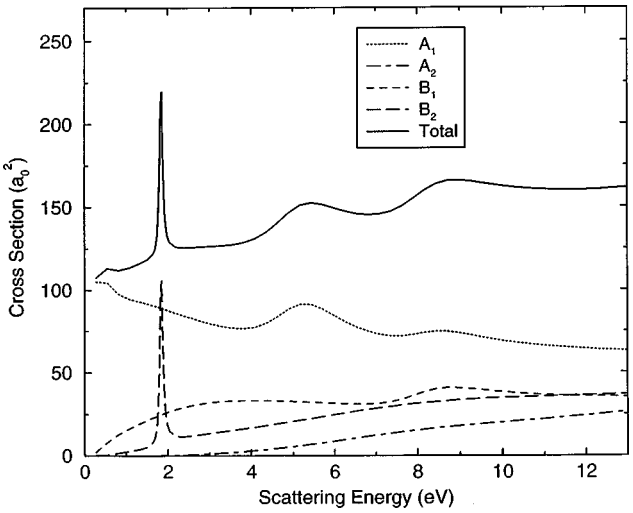

FIG. 1. Static exchange partial and total cross sections for e^--BCl_3 scattering.

calculations, as the SE cross section is a well-defined quantity, independent of the method used to perform the calculation.

In Fig. 1 the static exchange results are shown by (C_{2v}) symmetry. The most prominent feature is the resonance appearing in the B_2 symmetry at about 2 eV. This resonance is a classic temporary negative-ion shape resonance—the target SCF calculation also shows an unoccupied orbital of b_2 symmetry with an orbital energy of $\sim$2 eV. Since BCl_3^- is bound [BCl_3 has an electron affinity (EA) of about 0.3 eV [16,33]], we might expect this resonance to be an artifact of the static-exchange approximation and to vanish when we include correlation effects. However, the equilibrium geometries of BCl_3 and BCl_3^- are quite different, planar (D_{3h}) and tetrahedral (C_{3v}), respectively. Baeck and Bartlett [16] calculated a *vertical* EA of -0.41 to -0.64 eV, depending on the basis set and the method used. That is, these many-body perturbation theory calculations show BCl_3^- at an energy above BCl_3 in the equilibrium geometry of BCl_3. Thus we should expect that the position of this resonance should be lower in calculations including the effects of closed channels than it is at the SE level, but that it should not disappear, since our calculations are carried out at the ground-state geometry of BCl_3.

As with most SE calculations, the scattering amplitude associated with the totally symmetric irreducible representation (here A_1) is not expected to behave even qualitatively correctly as the scattering energy approaches zero. This symmetry contains the scattering functions with partial wave $l=0$, which penetrate the target even at low energies. At low energies the closed channel $(N+1)$-electron configurations are critical to induce the long-range interaction due to target polarization. Two broad shape resonances appear in A_1 symmetry at about 5.5 and 8.5 eV. The latter appears in B_1 as well. It is generally the case that such resonances drop in energy when correlation effects are included. The A_2 cross section is featureless.

B. Polarized SCF

To describe the scattering at low energies, we need an accurate representation of correlation and polarization. The sum in Eq. (1) incorporates dynamic target polarization and distortion effects into the Kohn trial function by including $(N+1)$-electron configuration state functions (CSF's), Θ_i, constructed from the product of bound molecular orbitals and terms obtained by singly exciting the target SCF wave function. Thus the configurations Θ_i in Eq. (1) have the form

$$\Theta_i = A(\chi_o[\varphi_o \rightarrow \varphi_\alpha]\varphi_i), \tag{4}$$

where $\varphi_o \rightarrow \varphi_\alpha$ denotes the replacement of occupied orbital φ_o by orbital φ_α and φ_i is another virtual orbital. Instead of using all the unoccupied orbitals to define a space of singly excited CSF's, we choose a compact subset of these virtual orbitals, the polarized virtual orbitals, denoted by φ_α in Eq. (4), for singly exciting the target. The polarized-SCF model has previously been shown (in calculations on CH_4 [20], SiH_4 [21], CF_4 [22], and C_2H_6 [34]) to provide a quantitatively accurate treatment of target polarization while maintaining a balanced description of correlation in the N- and $(N+1)$-electron systems. The polarized orbitals [20] are defined in first-order perturbation theory from the linear response of the target SCF wave function to an externally applied electric field. In general, there will be three polarized orbitals, one for each Cartesian component of the dipole operator (μ_α), for every occupied SCF orbital treated in this manner. In practice, the orbitals are obtained by diagonalizing the operator

$$P_{ij}^{\alpha} = \frac{\langle \varphi_i | \mu_\alpha | \varphi_o \rangle \langle \varphi_o | \mu_\alpha | \varphi_j \rangle}{(\varepsilon_i - \varepsilon_o)(\varepsilon_j - \varepsilon_o)} \tag{5}$$

in the space of ''improved virtual orbitals'' (IVO's), φ_i, which are eigenfunctions of the V_{N-1} Fock operator,

$$F_{\mathrm{IVO}} = h + 2J_C - K_C + J_o + K_o \tag{6}$$

with eigenvalues ε_i; ε_o is the closed-shell Hartree-Fock eigenvalue of the orbital being polarized. In Eq. (6), h is the sum of the one-electron kinetic energy and electron-nuclear attraction operators, J_C and K_C are the Coulomb and exchange operators for the doubly occupied target orbitals, and J_o and K_o are the Coulomb and exchange operators for the orbital being polarized. Further details are given elsewhere [20].

Treating the highest nine SCF orbitals in this manner generates 27 polarized orbitals. Taking single excitations from these nine SCF orbitals into the polarized orbitals gives a polarizability of 8.75 Å^3, 93% of the experimentally determined value of 9.38 Å^3 [35]. This level of agreement indicates that scattering from an SCF target should be a reasonable approximation.

Figure 2 shows the polarized-SCF cross sections by symmetry. Note the very large A_1 cross section as the scattering energy approaches zero. Upon examination we find that one of the A_1 eigenphases approaches nearly $\pi/2$ in this limit, consistent with a (near) zero energy virtual state. To verify this interpretation of our result, we performed additional calculations for the A_1 cross section in which the strength of our optical potential V_{opt} was artificially increased or decreased by a constant scale parameter. On decreasing the potential strength, this eigenphase approaches zero; on increasing, it approaches π. Levinson's theorem identifies this behavior as

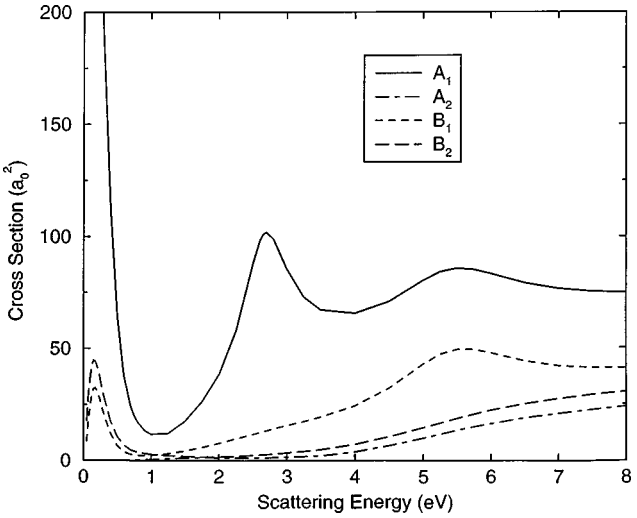

FIG. 2. e^--BCl_3 partial cross sections in the polarized-SCF treatment.

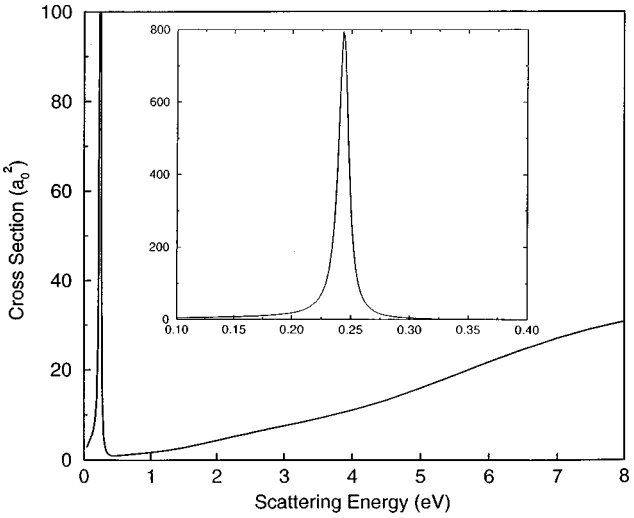

FIG. 3. Resonant B_2 cross section in the relaxed-SCF treatment. Inset shows low-energy detail.

the appearance of a bound state. The limit $\pi/2$ is associated with a zero-energy virtual (or bound) state, and with an infinite zero-energy cross section. Of course, our calculations cannot be performed exactly at zero energy. While the calculated cross section just above threshold is expected to be accurate, the value at threshold is shown by the numerical experiment described above to be extremely sensitive to correlation effects. We can obtain a rough estimate of the position of the virtual state by subjecting the A_1 eigenphase sum (which is *s*-wave dominated at low energies) to a modified effective range theory (MERT) analysis. For electron scattering from a polarizable target, the cotangent of the *s*-wave phase shift may be expanded about $k=0$ as [36]

$$k \cot \delta_0 = -\frac{1}{A} + Bk + Ck^2 \ln k + Dk^2 + \cdots , \qquad (7)$$

where A is the scattering length and B, C, and D may be taken as parameters. In the case where there exists a near zero-energy bound or virtual state, it is more appropriate to make the MERT expansion about the associated pole at $k = i\gamma$ [36],

$$k \cot \delta_0 = -\gamma + F(\gamma^2 + k^2) + \cdots . \qquad (8)$$

If γ is small, then it is related to the scattering length by $1/A = \gamma$. We have performed a number of fits of our A_1 eigenphase sums to Eqs. (7) and (8), varying the number of data points and the number of terms kept in Eq. (7). All fits give a negative scattering length A, consistent with the existence of a virtual state. The smallest (in absolute value) scattering length we found was $A \approx -10a_0$. Fits to Eq. (8), the expansion about the pole, consistently put the virtual state closer to zero energy, with $A \approx -200a_0$, corresponding to a virtual state near 0.4 meV.

The polarized-SCF A_1 cross section still shows two broad resonances at 2.5 and 5.5 eV, the resonance positions having dropped from their SE values, as expected. The B_1 symmetry also contains the 5.5 eV feature; the A_2 cross section is still structureless.

The B_2 cross section, while showing some enhancement below 1 eV, does not display the characteristics of a true resonance (the B_2 eigenphase sum does not change by π in this energy range). Examination of the trial wave function showed that the polarized-SCF treatment has overcorrelated the negative ion in B_2 symmetry by actually binding the extra electron. Since there is theoretical [16] and experimental [33] evidence that this resonance should appear at a few tenths of an eV, a different approach to scattering in this symmetry is required. In the next section, we apply a level of correlation more appropriate to the temporary negative-ion state.

C. Relaxed SCF

The B_2 symmetry contains the temporary negative-ion resonance, which corresponds to the temporary capture of the incident electron into an empty b_2 valence orbital. Because this orbital is localized in the region of space where there is significant target charge density, we expect that its temporary occupation will lead to a significant relaxation of the remaining occupied molecular target orbitals and a consequent lowering of the resonance energy. To account for this relaxation, we use an approach—the relaxed-SCF model—that has been shown to be successful for similar resonances in N_2 [23], H_2CO [24], C_2H_4 [25], and N_2O [37]. The key is to include in the trial function only those $(N+1)$-electron correlation terms that produce an orbital relaxation effect of the type that would be produced in performing an SCF calculation on the negative ion [38]. Thus, the configurations that we include in the set Θ_i are built only from singlet-coupled, single excitations of the occupied target orbitals into virtual orbitals *of the same symmetry*. We do not include any configurations that break the spatial or spin symmetry of the ground state. This type of core relaxation mimics an SCF calculation on the negative ion in this symmetry. In the polarized-SCF model, by contrast, the dominant effect included is the dynamic distortion of the target orbitals through single excitations into a set of virtual orbitals that are optimized to reproduce the target polarizability. We include excitations from a given occupied orbital into all the

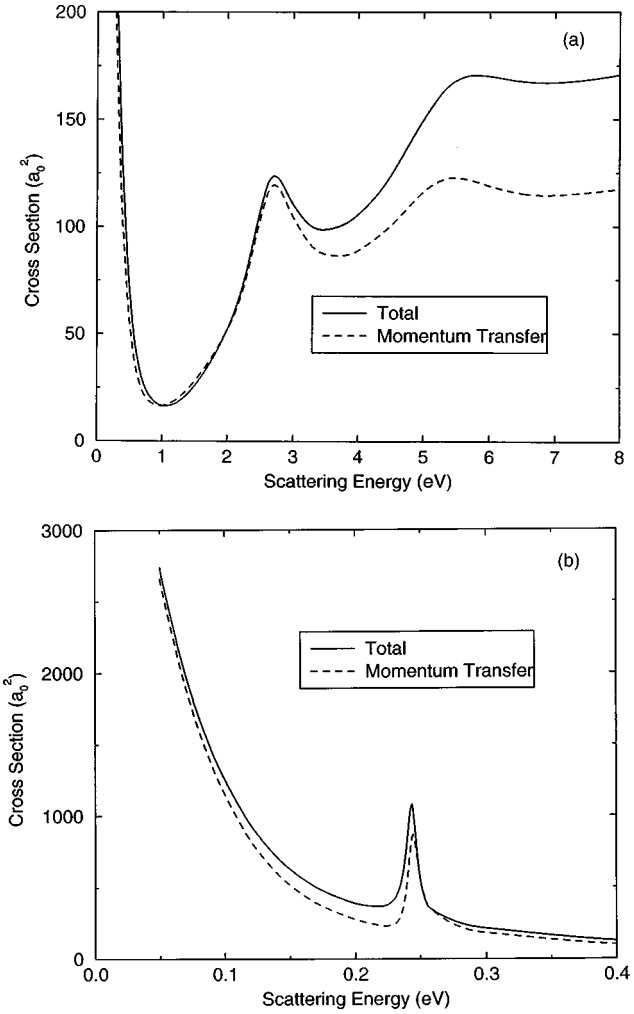

FIG. 4. Total and momentum transfer cross sections for e^--BCl_3 scattering (a) below 8 eV and (b) showing the B_2 resonance.

polarized orbitals, irrespective of symmetry, and include both singlet and triplet intermediate spin couplings. While such a model does incorporate long-range polarization effects into the trial function, the polarized-SCF model evidently also leads to an overcorrelation of the target at short range and unphysical binding of the negative ion in this symmetry. The relaxed-SCF model, by contrast, includes a more appropriate treatment of short-range target distortion in a way that does not recorrelate the target SCF wave function. Again, this approach allows the target wave function to relax in the field of the scattering electron while retaining the resonant scattering symmetry.

In Fig. 3 we show the B_2 cross section in the relaxed-SCF treatment. The resonance does appear at 0.25 eV, with a width of only 10 meV. Note that above the resonance, the relaxed-SCF and polarized-SCF B_2 cross sections are quite similar. This similarity confirms our expectation that correlation effects are most important at the lowest scattering energies, and that any reasonable treatment of correlation is adequate at energies above a few eV.

D. Integral and differential cross sections

In Fig. 4 we show the total and momentum transfer cross sections, using the polarized-SCF treatment for A_1, A_2, and B_1 symmetries, and the relaxed-SCF treatment for B_2. The sharp B_2 resonance lies embedded in the wing of a strongly rising A_1 background cross section as $E \rightarrow 0$, reflecting the presence of an unbound virtual state. These are our best values for the cross sections from the calculations presented in this work.

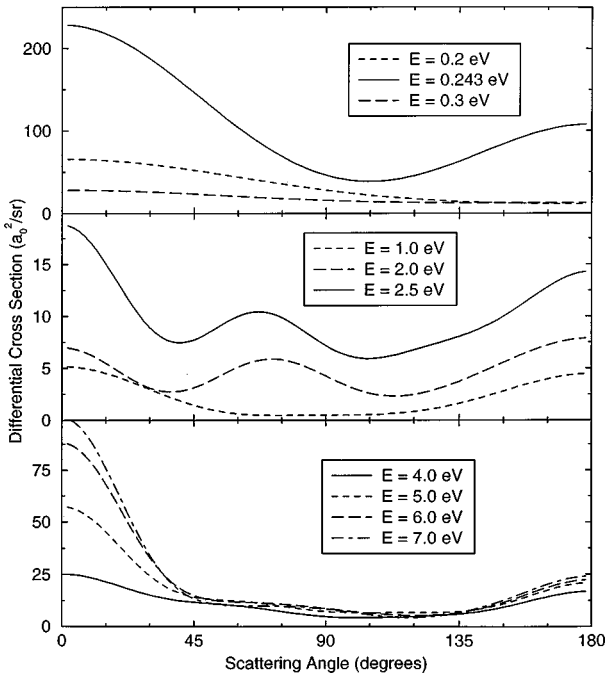

FIG. 5. Differential cross sections for e^--BCl_3 scattering at several scattering energies.

Figure 5 shows the differential cross section (DCS) at several energies. The top frame shows the DCS below, at the peak of, and above the B_2 resonance. This resonance shows primarily *p*-wave character, though its asymmetry about 90° indicates that other angular momenta contribute. The DCS in the 2.5 eV resonance shows more *d*-wave character, but again there is strong mixing. As the scattering energy increases, the DCS becomes more forward peaked.

Numerical values of all cross sections presented in this work are available from the authors on request.

IV. DISCUSSION

In summary, we have presented the results of large-scale complex Kohn variational calculations on electron-BCl_3 scattering, including the effects of target distortion through the use of a set of polarized orbitals to include the effects of energetically closed channels in an *ab initio* fashion, and using a treatment appropriate to the temporary negative-ion resonance. This is, to our knowledge, the only published determination of the elastic cross sections for BCl_3, experimental or theoretical.

While measured elastic cross sections are not available to compare with our results, we can address the consistency of our findings with some of the known inelastic results. The threshold for dissociative attachment is about 1 eV [11] and in fact peaks somewhere near this value. We conclude that the negative-ion B_2 resonance at 0.25 eV is therefore *not* a precursor for this process, since it lies energetically below

the BCl_2+Cl^- limit. The lower of the two broad A_1 resonances found in our polarized-SCF calculations is a more likely candidate for DA. The B_2 resonance and the large zero-energy cross section are, however, consistent with the large attachment rates (presumably leading to BCl_3^-) seen in swarms, which indicate that the attachment cross section peaks at or near zero energy. These fixed-nuclei calculations do not allow us to calculate an autodetachment lifetime for the temporary negative-ion state, as this (apparently quite long) lifetime is surely dependent on nuclear dynamics.

Our momentum transfer cross sections should be of use in a Boltzmann analysis of swarm measurements. Our results should also serve as a base reference for future studies on electron-BCl_3 scattering.

ACKNOWLEDGMENTS

We would like to acknowledge useful discussions on BCl_3 kinetics with W. L. Morgan (Kinema Research). This work was performed under the auspices of the U.S. Department of Energy by the Lawrence Berkeley National Laboratory and the Lawrence Livermore National Laboratory under Contract Nos. DE-AC03-76F00098 and W-7405-Eng-48, respectively. Computer time and assistance was supplied by the National Energy Research Scientific Computing Center.

[1] D. Flamm, Solid State Technol. **36**, 49 (1993).
[2] S. J. Pearton, W. S. Hobson, C. R. Abernathy, F. Ren, T. R. Fullowan, A. Katz, and A. P. Perley, Plasma Chem. Plasma Process. **13**, 311 (1993).
[3] R. H. Burton, R. A. Gottscho, and G. Smolinsky, *Dry Etching for Microelectronics*, edited by R. A. Powell (Elsevier, New York, 1984).
[4] G. J. Sonek and J. M. Ballantyne, J. Vac. Sci. Technol. B **2**, 653 (1984).
[5] I. Tokue, M. Kudo, M. Kusakabe, T. Honda, and Y. Ito, J. Chem. Phys. **96**, 8889 (1992).
[6] Z. J. Jabbour, K. E. Martus, and K. Becker, Z. Phys. D **9**, 263 (1988); P. G. Gilbert, R. B. Siegel, and K. Becker, Phys. Rev. A **41**, 5594 (1990).
[7] C. Q. Jiao, R. Nagpal, and P. Haaland, Chem. Phys. Lett. **265**, 239 (1997).
[8] R. Nagpal and A. Garscadden, Appl. Phys. Lett. **64**, 1626 (1994).
[9] D. L. Mosteller, Jr., M. L. Andrews, J. D. Clark, and A. Garscadden, J. Appl. Phys. **74**, 2247 (1993).
[10] L. J. Overzet and L. Luo, Appl. Phys. Lett. **59**, 161 (1991).
[11] Z. Lj. Petrović, W. C. Wang, M. Suto, J. C. Han, and L. C. Lee, J. Appl. Phys. **67**, 675 (1990).
[12] G. R. Scheller, R. A. Gottscho, T. Intrator, and D. B. Graves, J. Appl. Phys. **64**, 4384 (1988).
[13] J. A. Stockdale, D. R. Nelson, F. J. Davis, and R. N. Compton, J. Chem. Phys. **56**, 3336 (1972).
[14] I. S. Buckel'nikova, Zh. Eksp. Teor. Fiz. **35**, 1119 (1958) [Sov. Phys. JETP **8**, 783 (1959)].
[15] J. Olthoff, Ph.D. dissertation, University of Maryland, 1985 (unpublished).
[16] K. K. Baeck and R. J. Bartlett, J. Chem. Phys. **106**, 4604 (1997).
[17] T. N. Rescigno, B. H. Lengsfield III, and C. W. McCurdy, in *Modern Electronic Structure Theory*, edited by D. R. Yarkony (World Scientific, Singapore, 1995), p. 501.
[18] T. N. Rescigno, C. W. McCurdy, A. E. Orel, and B. H. Lengsfield III, in *Computational Methods for Electron-Molecule Collisions*, edited by W. M. Huo and F. A. Gianturco (Plenum, New York, 1995), p. 1.
[19] H. Feshbach, Ann. Phys. (N.Y.) **5**, 357 (1958); **19**, 287 (1962).
[20] B. H. Lengsfield III, T. N. Rescigno, and C. W. McCurdy, Phys. Rev. A **44**, 4296 (1991).
[21] W. Sun, C. W. McCurdy, and B. H. Lengsfield III, Phys. Rev. A **45**, 6323 (1992).
[22] W. A. Isaacs, C. W. McCurdy, and T. N. Rescigno, Phys. Rev. A **58**, 309 (1998).
[23] A. U. Hazi, T. N. Rescigno, and M. Kurilla, Phys. Rev. A **23**, 1089 (1981).
[24] T. N. Rescigno, C. W. McCurdy, and B. I. Schneider, Phys. Rev. Lett. **63**, 248 (1989).
[25] B. I. Schneider, T. N. Rescigno, B. H. Lengsfield III, and C. W. McCurdy, Phys. Rev. Lett. **66**, 2728 (1991).
[26] A. P. P. Natelense, M. H. F. Bettega, L. G. Ferreira, and M. A. P. Lima, Phys. Rev. A **52**, R1 (1995).
[27] T. N. Rescigno and C. W. McCurdy, J. Chem. Phys. **104**, 120 (1996).
[28] T. N. Rescigno, J. Chem. Phys. **104**, 125 (1996).
[29] T. N. Rescigno, A. E. Orel, and C. W. McCurdy, Phys. Rev. A **56**, 2855 (1997).
[30] L. F. Pacios and P. A. Christiansen, J. Chem. Phys. **82**, 2664 (1985).
[31] T. H. Dunning, J. Chem. Phys. **53**, 2823 (1970).
[32] T. N. Rescigno and A. E. Orel, Phys. Rev. A **43**, 1625 (1991).
[33] E. W. Rothe, B. P. Mathur, and G. P. Reck, Inorg. Chem. **19**, 829 (1979).
[34] W. Sun, C. W. McCurdy, and B. H. Lengsfield III, J. Chem. Phys. **97**, 5480 (1992).
[35] A. N. M. Barnes, D. J. Turner, and L. E. Sutton, Trans. Faraday Soc. **67**, 2902 (1971).
[36] T. F. O'Malley, L. Spruch, and L. Rosenberg, J. Math. Phys. **2**, 491 (1961).
[37] C. Winstead and V. McKoy, Phys. Rev. A **57**, 3589 (1998).
[38] B. I. Schneider and P. J. Hay, Phys. Rev. A **13**, 2049 (1976).